Proc. of the 8th International Symposium on Geotechnical Safety and Risk (ISGSR)
Edited by Jinsong Huang, D.V. Griffiths, Shui-Hua Jiang, Anna Giacomini and Richard Kelly
©2022 ISGSR Organizers. *Published by* Research Publishing, Singapore.
doi: 10.3850/978-981-18-5182-7_06-001-cd

Reliability Analysis of Width-Constrained Piled Slopes Considering Three-Dimensional Spatial Variability of Soil Strength

Zhibin Sun[1], Hao Zhuang[1], Daniel Dias[2], Tingting Zhang[2]

[1]School of Automotive and Transportation Engineering, Hefei University of Technology
[2]Laboratory 3SR, University Grenoble Alpes

Abstract: Stabilization pile is a common measurement to enhance slope stability. Since the deterministic factor of safety cannot reflect the inherent uncertainty and spatial variability of mechanical properties of soil, it is highly desirable to employ a probabilistic analysis for slope reinforced with piles. This paper presents a probabilistic analysis procedure for width-constrained piled slope where the failure pattern and spatial variability of soil are both accounted for under three-dimensional (3D) conditions. A modified discretization kinematic analysis-based mechanism is employed as the determined model. Such a mechanism adopts a novel hybrid strategy to greatly improve the computational efficiency on the basis of the origin discretization mechanism. The effective cohesion and friction angle of the soils are modeled as lognormal random fields by using the Karhunen–Loève expansion. The sparse polynomial chaos expansion (SPCE) is used to construct the metamodel to reduce huge computation costs in high dimensional stochastic problems. The failure probabilities, probability density function and other useful reliability results can be provided within limited simulations. Finally, the influences of soil spatial variability, slope geometry and pile parameter on reliability analysis results are conducted. The combination of modified discretization mechanism and SPCE provides a useful tool in probabilistic analysis of piled slope under 3D conditions. The reliability finding is also helpful for piled slope reliability design in practice.

Keywords: pile reinforced slope; three-dimensional reliability analysis; soil spatial variability; kinematic analysis; sparse polynomial chaos expansion

1 Introduction

Anti-sliding piles are widely used in slope reinforcement to improve stability, due to the advantages of strong stability, easy construction and little disturbance to the original slope (Cai 2000; Won et al. 2005).

Many studies have been contributed to developing stability approach of piled slopes and/or to investigate the effect of pile design parameters on piled slope stability (Ausilio 2001; Li 2006; Nian et al. 2008). However, the results of stability analysis do not always agree with the situation in practice. For instance, a slope with "higher" safety factor may have a greater probability to failure (Li et al. 2015; Huang et al. 2019). This is because the huge uncertainties and randomness of geological and soil parameters, usually due to inadequate site characteristics, measurement errors, etc., cannot be considered by stability analysis. To deal with these 'statistical characteristic' of soil properties, a reliability analysis is essential, which allows a systemic and quantitative description of the probability of slope failure. Reliability analysis of pile-reinforced slope receives an increasing attention in past decade (Li 2014; Zhang et al. 2017). A simple treatment of soil parameter uncertainty is to assume that the soil parameters are random variables and are homogeneous across the site. However, this assumption is not realistic because of inherent spatial variability of soil parameters due to mineral composition, deposition conditions, and stress history (Qi 2018; Chen 2019). Failure to consider spatial variation in probabilistic analysis results in overestimated failure probabilities and uneconomic designs (Guo 2019). Thus, some scholars considered spatial variability in the reliability analysis of reinforced slopes. Chen et al. (2020) analyzed the effects of pile positions, pile lengths on the failure probability of reinforced slopes of soil strength spatial variability. Considering the spatial variability of soil parameters and the uncertainty of stabilized piles, Lü et al. (2021) performed a probabilistic analysis of the reinforced slopes. However, most of the reliability analyses of reinforced slopes considering spatial variability are based on two-dimensional analyses and not, to the best of our knowledge, under three-dimensional condition. A contrary fact is that in practice slope failures often illustrate obvious 3D characteristics, for instance, a slope with limited width due to adjacent rock formation or artificial excavation. An arbitrary 2D reliability analysis of such slope will lead an overestimation of the failure probability. Moreover, a reliability design that takes the overly overestimated results will increase the unnecessary cost in engineering practices, such as excessive reinforcement or excavation. To acquire the more realistic probabilistic results, 3D reliability analysis is necessary. The determination model is essential for reliability analysis, practically for the three-dimensional analysis since 3D analysis is often more time-consuming than 2D ones.

Serval methods have been used in the reliability analysis of reinforced slopes, such as limit equilibrium method (LEM) (Tabarroki et al. 2013; Gravanis 2014), finite element method (FEM) (Griffiths 2011; Dyson 2019),

finite difference method (FDM) (Srivastava 2012; Li et al. 2017). However, there are some problems when LEM and numerical approach FEM/FDM is applied in 3D spatial variability issues. LEM needs to introduce some arbitrary assumptions to determine the inter-piece forces, where soil variability and boundary conditions are hard to account for in a systematic way. For FEM and FDM, expensive time costs hinder their use for massive computation. Apart from these two approaches, kinematic analysis based on limit analysis is considered a sound stability method used as determination model. A horn-like 3D mechanism based on kinematic analysis has been successfully applied to stability analysis of reinforced slopes. However, this mechanism cannot consider the spatial variability of friction angle due to the requirements of normal conditions.

To address that, this paper adopts an improved 3D discretization mechanism based on this horn-like mechanism. This mechanism, of which the sliding surface consists of several triangular discrete unit surfaces, can consider the spatial variability of soil parameters. By the combination of the 3D discretization mechanism and the random field theory, the reliability of the 3D pile reinforced slope considering the spatial variability of soil parameters is analyzed in this paper. In addition, a large number of input variables are required in random field problem. As the high-dimensional stochastic problems are time-consuming, a meta-models called sparse polynomial chaos expansion (SPCE) are used to improve computational efficiency.

In summary, this paper aims to propose a 3D reliability analysis method for reinforced slopes considering spatial variability, by using the SPCE method and the 3D discretization mechanism. It is also investigated the effects of some key parameters such as auto correlation distance, coefficient of variation, pile position, pile spacing, and width-to-height ratio on the failure probability of 3D reinforced slopes.

2 Random field model

A random field model is used to replicate the spatial variability of soil strength properties, by defining a continuous parameter field with a set of random variables. Stochastic distribution (mean, variance, etc) and autocorrelation function completely describe a random field model.

This study assumes the cohesion and friction follow log-normal distribution and autocorrelation function is exponential. The exponential autocorrelation function can be expressed as

$$C[(x_1,y_1,z_1),(x_2,y_2,z_2)] = \exp(-\frac{|x_1-x_2|}{l_x}-\frac{|y_1-y_2|}{l_y}-\frac{|z_1-z_2|}{l_z}) \tag{1}$$

where (x_1,y_1,z_1) and (x_2,y_2,z_2) are the coordinates of two arbitrary points in the 3D random field space, l_x, l_y, and l_z are the autocorrelation distances in the x, y, and z directions, respectively.

A discretization process is necessitated in dealing with random field problem. In this paper, a Karhunen-Loeve expansion is utilizing to realize the random field discretization, due to its efficiency and the merit that the number of required random variables is not affected by the mesh division.

The K-L expansion of a log-normal random field can be expressed as:

$$\widehat{R}(x,y,z,\theta) \approx \exp[\mu_{\ln} + \sigma_{\ln}\sum_{i=1}^{M}\sqrt{\lambda_i}\phi_i(x,y,z)\xi_i(\theta)] = \exp[\mu_{\ln} + \sigma_{\ln}G(x,y,z,\theta)] \tag{2}$$

where λ_i and ϕ_i are the i-th eigenvalue and eigenfunction of the autocorrelation function, respectively. $\xi_i(\theta)$ denotes the coordinates of the realization of the random filed in the expanded space. M is the number of series expansion terms, $\mu_{\ln}$ and $\sigma_{\ln}$ are the normalized mean and standard deviation of random filed.

3 Sparse polynomial chaos expansion(SPCE)

Sparse polynomial chaos expansion（SPCE） proposed by Blatman and Sudret (2008) is an extension of Polynomial chaos expansion. PCE is a meta modelling tool that expands the model response on a suitable basis to approximate a complex deterministic model.

A PCE with the number of random variables can be expressed as

$$M_p(X) = \sum_{0\le|\alpha|\le \mathrm{p}} a_\alpha \psi(X), \quad |\alpha| \equiv \sum_{i=1}^{M}\alpha_i \tag{3}$$

where X is the independent random variable; M is the number of random variables; $\psi(X)$ is a multivariate polynomial that can be expressed as a tensor product of univariate orthogonal polynomials; a_α is the unknown coefficients; $\alpha=\{\alpha_1,\ldots,\alpha_M\}$ is a multidimensional index and p is the order of the expansion. SPCE aims to reduce the number of the involved multivariate polynomials by selecting the terms with the significant coefficients.

4 Three-dimensional anti-slip pile reinforced slope limit analysis

4.1 Three-dimensional discrete slope failure mechanism

A limit analysis-based mechanism proposed by Michalowski is an efficient approach for assessing stability of 3D slopes. This mechanism, which processes a log-spiral failure plane, has been employed to investigate the stability problem with 3D piled slopes. This mechanism, however, is unavailable in present study, since its log-spiral counter is not kinematic admissible for friction angle spatially varying slope due to the normal condition of associated flow rule. For this reason, a modified Michalowski's mechanism based on the failure plane discretization is employed as the determination model in this paper. Unlike the traditional mechanism, its velocity discontinuity plane is discretized into a series of triangular elements.

The generation of these discretization elements dependent on 'point-by-point' technique that rigorously obeys the associated rule flow, which makes the improved mechanism has good applicability for accounting for spatially variation of friction angle. The profile of the discretization mechanism is plotted in Figure 1. It describes a rotating failure with sliding plane passing through the slope toe. Mechanism generation is conducted with the help of a series of radial planes Π_1, Π_2, which are perpendicular to lateral plane of slopes through the rotation axis OO', any adjacent planes having constant angle $\delta\theta$. Assume that all discretization points $A_{i,j}$ are positioned on these radial planes, where j denotes the radial plane where the point is positioned and i denotes the position of points on the given plane. The discretization points $A_{i,1}$ on the first radial plane Π_1 uniformly arrange in an ellipse. The adjacent lines $E_0A_{i,1}$ and $E_0A_{i+1,1}$ have constant angle η, where E_0 is intersection point of plane Π_1 and the center line of curved conic FDD'. Concerning more details about the curved conic FDD', readers can refer to Mollon (2011).

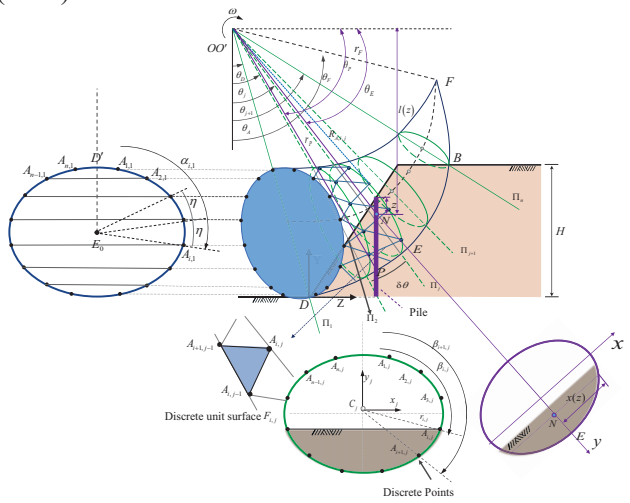

Figure 1. Schematic diagram of the improved 3D discrete mechanism

Generation of discretization points is based on the principle that point $A_{i,j}$ on the plane Π_j is deduced from two adjacent points $A_{i,j-1}$ and $A_{i+1,j-1}$ on previous plane Π_{j-1}.The generation process starts by determining the point $A_{i,2}$ on the plane Π_2 from the point on the plane Π_1, followed by determining the points on Π_3 from those on $\Pi_2\cdots$, clockwise along each plane in turn. The derivation of a new point follows two principles described below.(1) The plane of discretization element $F_{i,j}(A_{i,j-1},A_{i+1,j-1},A_{i,j})$ is at an angle φ_i with its velocity vector $\vec{v}_{i,j}(X_{v,i,j},Y_{v,i,j},Z_{v,i,j})$. This is because kinematic analysis theory necessitates a sliding plane respecting the normal condition, to achieve a kinematical admissibility in the whole mechanism.(2) The distances from the new point $A_{i,j}$ to the known points $A_{i,j-1}$ and $A_{i+1,j-1}$ are approximately equal. This is not a necessity for the normal condition, but it allows for a quasi-uniformly distribution of discretization points.

4.2 Mechanism energy calculation and solution process

Calculations of external work of the mechanism are conducted by summation of elementary rates as shown in Figure 2.

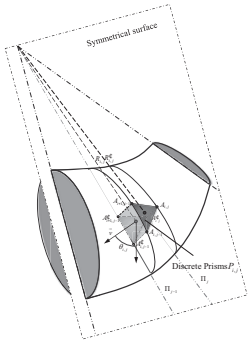

Figure 2. Schematic diagram of energy consumption calculation for horn failure mechanism

The power rates due to gravity can be expressed as following:

$$W = \gamma \sum_{i,j} (R_{i,j} V_{i,j} \cos\theta_{i,j}) \tag{4}$$

where γ is soil weight, and $V_{i,j}$ is the volume of prism $P_{i,j}$, $R_{i,j}$, $\theta_{i,j}$and $P_{i,j}$ can be found in Figure 2.

Computation of energy dissipation rate follows the same principle as work rates.

$$D_{3D} = \omega \sum_{i,j} (c_{i,j} R'_{i,j} S_{i,j} \cos\varphi_{i,j}) \tag{5}$$

where $S_{i,j}$ is the area of $F_{i,j}$; $c_{i,j}$ and $\varphi_{i,j}$ are the cohesion and the friction angle at the center of $F_{i,j}$, respectively. $R'_{i,j}$ can be found in Figure 2.

Energy dissipation rate caused by the anti-sliding pile can be expressed as

$$D_{\mathrm{p}} = 2\omega \int_0^h \frac{p(z)}{D_1} x(z) l(z) \mathrm{d}z \tag{6}$$

where $x(z)$ is half of the width of the failing soil at point z, $l(z)$ is the vertical distance from any point z on the pile to rotation axis OO'. D_1 is the center distance of two adjacent anti-sliding piles; D_2 is the distance between the edges of two adjacent anti-sliding piles small distance; $d_p = D_1 - D_2$ is the diameter of the anti-slide pile. Readers can refer to Gao (2015) for more details on the energy calculation of anti-slip piles.

After building the equation of work rate and energy dissipation, the optimal upper bound solution of the safety factor can be calculated along with the combination of the dichotomy method and the strength reduction method. Readers can refer to Sun et al. (2018) for more details about the calculation of safety factor.

5 Parameter Analysis

This section conducts a parametric analysis to investigate the effect of spatial variability (l_x, l_y, l_z, COVc, COVφ) and the slope design parameters (X_F / L_X, D_1 / d_p, B / H) on the reliability results of pile-reinforced slope with width constrained, using the 3D discretization kinematic analysis model together with the SPCE meta-model technique. The basic parameters are as follows: The mean value of cohesion c is 10 kPa and its variation coefficient is 30%. The mean value of friction angle φ is 20° and its variation coefficient is 20%. The vertical and horizontal auto correlation distance is 2m and 20m, respectively. The slope height H is 10m, the ratio of width to height B / H is 2, the slope inclination β is 45°, and the soil weight γ is 17kN / m^3. The pile position parameter X_F / L_X is 0.8, the pile spacing D_1 / d_p is 2.5.

5.1 Influence of auto correlation distance

Figure 3 presents the influence of the vertical auto correlation distance(l_y) on the probability density function(PDF) and failure probability(P_f). Several typical values of auto correlation distance are considered: l_y =1m, 2m and 4m and $l_x = l_z$=20m.The other parameters are remains as their reference value. Figure 3 illustrates that the PDF curves have taller and narrower shape with the increasing of l_y .This means that the variability of safety factor of 3D reinforced slope decreases when soil spatial heterogeneity is more significant in vertical direction.

Figure 4 indicated the effect of horizontal auto correlation distance on PDF and P_f . The similar conclusion can be drawn in Figure 4. From a physical point of view, larger auto correlation distances imply a stronger correlation of soil properties between discrete points and therefore a greater probability of producing a more homogeneous soil during random field generation. This indicates that larger auto correlation distances cause a higher variation of the calculated safety factor, because in that case mean value of the soil parameters significantly change in each realization in random field.

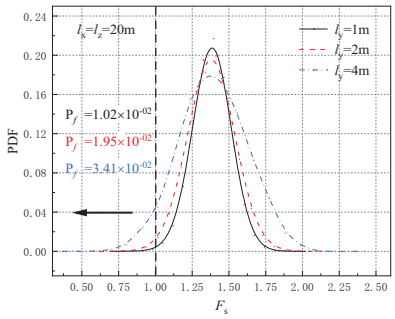

Figure 3. PDF of safety factor under different l_y

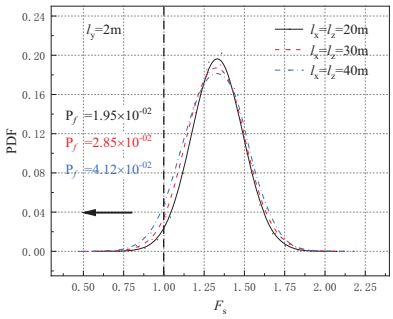

Figure 4. PDF of safety factor under different l_x and l_z

The observation also means that on sliding surface the fluctuation of soil parameters is more significant with smaller auto correlation distances, and the simulated values are averaged to the mean value along the slip surface. This is the reason why the smaller the auto correlation distance results in the failure probability. For example, the failure probability decreases from 3.41 × 10^{-2} to 1.02 × 10^{-2} when l_y varies from 4 to 1 m with l_x and l_z being 20 m).In addition, it is known from Figure 3 and Figure 4 that PDF curve is subject to greater fluctuation with l_y than with l_x and l_z,.This means that l_y give a more impact on the probability results.

5.2 Influence of variation coefficient on failure probability

Figure 5 shows the effect of COVc on P_f in the range of COVc=10% to 50%, where l_y=1m, 2m and 4m.It is found that P_f increases with the increase of COVc and its relative increment grows sharply with the increasing of COVc. For example, the failure probability increases from 2.24×10^{-4} to 1.95×10^{-2} by arising COVc from 0.1 to 0.3, increases from 1.95×10^{-2} to 1.39×10^{-1} with COVc from 0.3 to 0.5 when l_y is equal to 2m. This suggests that ignoring the spatial variability of soil parameters will overestimate the reliability of the slope and raises potential risk in slope engineering. Figure 5 also shows that lager vertical auto correlation distances lead to a great possibility of failure. This is consistent with the finding in the above section.

Figure 6 shows the effect of COVφ on P_f where COVφ ranges from 5% to 25% due to the variability of φ in practice is lower according to Luo (2016).Similar to Figure 5, Figure 6 shows that P_f grows when COVφ increases. In addition, a comparison of Figure 5 and 6 indicate that COVφ has a more significant effect on P_f than COVc. For example, P_f increases from 2.24×10^{-4} to 1.95×10^{-2} by arising COVc from 0.1 to 0.3, increases from 9.53×10^{-4} to 6.66×10^{-2} with COVφ from 0.05 to 0.25 when l_y is equal to 2m .

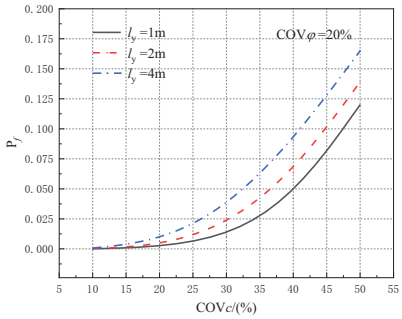

Figure 5. Influence of COVc on failure probability

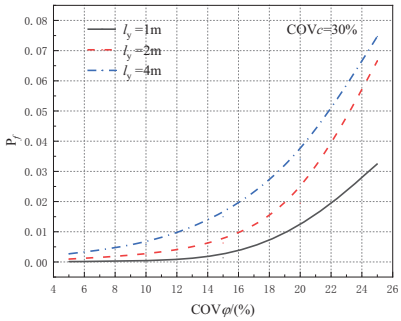

Figure 6. Influence of COVφ on failure probability

5.3 Effect of pile position X_F / L_X and pile spacing D_1 / d_p on the probability of failure

Figure 7 shows the effect of X_F / L_X（0, 0.25, 0.5, 0.75 and 1）on P_f of reinforced slope with different D_1 / d_p（1.5, 2 and 2.5）.It is found P_f decreases with X_F / L_X increasing from 0, reaches the minimum value when X_F / L_X equals to 0.6, and then increases as X_F / L_X varies from 0.6 to 1.This observation shows that the piles have the best reinforcement effect when X_F / L_X in the range of 0.5 to 0.75.

It also can be found that the pileless slope is basically in an unstable state (P_f is 69.1% at X_F / L_X=0) but when piles are installed at the most effective position, the risk of slope failure is slight(P_f is 5×10-6 around at X_F / L_X=0.5).This indicates that installation of the anti-slip pile at appropriate position can significantly reduce possibility of slope instability. Notice that the P_f is also relatively large when the X_F / L_X in the range of 0 to 0.25 or 0.85 to 1. This indicates that in practice the placement of piles should be carefully considered, otherwise the expected reinforcement effect will not be achieved. As expected, Figure 9 shows that P_f increases with increasing D_1 / d_p. It is worth noting that variation of D_1 / d_p has slight influence on the optimal installation position of the pile.

5.4 Effect of width-to-height ratio B/H on failure probability

Figure 8 shows the effect of B/H on P_f of reinforced slopes at different D_1/d_p.It is found that the failure probability increases with the increase of B/H .For example, the failure probability increases from 4.68×10-3 to 1.68×10-2 by improving B/H from 1 to 2.5 when D_1/d_p is equal to 2.5. B/H has an important influence on the reliability of slope stability, which corresponds to the observed decrease in the safety factor with increasing B/H (Pan 2017). It is noteworthy that the extent of change in P_f increases with increasing D_1/d_p. For instance, P_f increases by 6.1×10^{-5} , 2.8×10^{-3} and 1.2×10^{-2} respectively with B/H from 1 to 2.5 when D_1/d_p is equal to 1.5 , 2 and 2.5. For instance, the probability of failure increases by 6.1×10^{-5} , 2.8×10^{-3} and 1.2×10^{-2} respectively with B/H from 1 to 2.5 when D_1/d_p is equal to 1.5 , 2 and 2.5.More attention should be paid to piled slopes with larger D_1/d_p, when considering the increasing P_f due to the increasing of B/H .

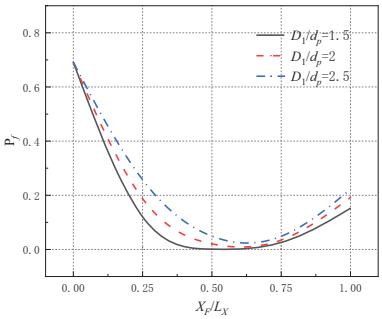

Figure 7. Effect of X_F/L_X on failure probability

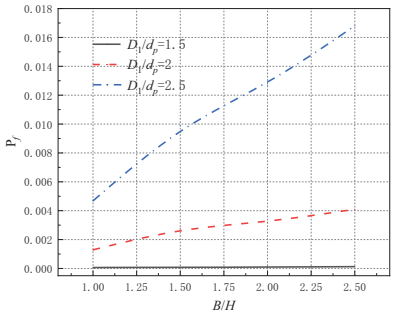

Figure 8. Effect of B/H on failure probability

6 Conclusions

In this paper, the reliability analysis of pile-reinforced slopes with width constrained is carried out with the consideration of spatial variability of soil strengths. The main conclusions are as follows.

1. The variability of safety factor, together with the failure probability of pile-reinforced slopes increases with the growth of auto correlation distance, in which the effects of l_y are greater than l_x and l_z.

2. The failure probability of pile-reinforced slope increases with the increase of the variation coefficient of cohesion and friction angle. Especially, P_f is more sensitive to the variation of friction angle than cohesion, in the given range of parameters.

3. Pile design parameters X_F/L_X and D_1/d_p has considerable influences on the failure probability of pile-reinforced slope. The change of P_f with X_F/L_X indicates that the effective position to install the pile is the middle of the slope surface ($X_F/L_X=0.6$). Placing the pile at a non-suitable position, for instance, on the bottom (1/4-1/3) of the slope surface, will lead in a failure of reinforcement from a failure probability view ($P_f>0.2$).

4. The failure possibility of pile-reinforced slope considerably increases with the slope width. It is recommended to consider the 3D effect in reliability assessment or reliability design when pile-reinforced slope is constrained in width.

References

Ausilio E, Conte E, Dente G. Stability analysis of slopes reinforced with piles[J]. *Computers and Geotechnics*, 2001, 28(8): 591-611.

Blatman G, Sudret B. Sparse polynomial chaos expansions and adaptive stochastic finite elements using a regression approach[J]. *Comptes Rendus Mécanique*, 2008, 336(6): 518-523.

Cai F, Ugai K. Numerical analysis of the stability of a slope reinforced with piles[J]. *Soils and foundations*, 2000,40(1): 73-84.

Chen F, Wang L, Zhang W. Reliability assessment on stability of tunnelling perpendicularly beneath an existing tunnel considering spatial variabilities of rock mass properties[J]. *Tunnelling and Underground Space Technology*, 2019, 88: 276-289.

Chen F, Zhang R, Wang Y, et al. Probabilistic stability analyses of slope reinforced with piles in spatially variable soils[J]. *International Journal of Approximate Reasoning*, 2020, 122: 66-79.

Dyson A P, Tolooiyan A. Prediction and classification for finite element slope stability analysis by random field comparison[J]. *Computers and Geotechnics*, 2019, 109: 117-129.

Gao Y, Ye M, Zhang F. Three-dimensional analysis of slopes reinforced with piles[J]. *Journal of Central South University*, 2015, 22(6): 2322-2327.

Gravanis E, Pantelidis L, Griffiths D V. An analytical solution in probabilistic rock slope stability assessment based on random fields[J]. *International Journal of Rock Mechanics and Mining Sciences*, 2014, 71: 19-24.

Griffiths D V, Huang J, Fenton G A. Probabilistic infinite slope analysis[J]. *Computers and Geotechnics*, 2011, 38(4): 577-584.

Guo X, Dias D, Pan Q. Probabilistic stability analysis of an embankment dam considering soil spatial variability[J]. *Computers and Geotechnics*, 2019, 113: 103093.

Huang D, Song Y X, Ma G W, et al. Numerical modeling of the 2008 Wenchuan earthquake-triggered Niumiangou landslide considering effects of pore-water pressure[J]. *Bulletin of Engineering Geology and the Environment*, 2019, 78(7): 4713-4729.

Li D Q, Jiang S H, Cao Z J, et al. Efficient 3-D reliability analysis of the 530 m high abutment slope at Jinping I Hydropower Station during construction[J]. *Engineering geology*, 2015, 195: 269-281.

Li L. Reliability based design for slope stabilization using drilled shafts and anchors[D]. *University of Akron*, 2014.

Li X P, He S M, Wang C H. Stability analysis of slopes reinforced with piles using limit analysis method[M]. *Advances in earth structures: research to practice*. 2006: 105-112.

Li X Y, Zhang L M, Gao L, et al. Simplified slope reliability analysis considering spatial soil variability[J]. *Engineering Geology*, 2017, 216: 90-97.

Lü Q, Xu B, Yu Y, et al. A practical reliability assessment approach and its application for pile-stabilized slopes using FORM and support vector machine[J]. Bulletin of Engineering Geology and the Environment, 2021: 1-13.

Luo N, Bathurst R J, Javankhoshdel S. Probabilistic stability analysis of simple reinforced slopes by finite element method[J]. Computers and Geotechnics, 2016, 77: 45-55.

Mollon G, Dias D, Soubra A H. Rotational failure mechanisms for the face stability analysis of tunnels driven by a pressurized shield[J]. International Journal for Numerical and Analytical Methods in Geomechanics, 2011, 35(12): 1363-1388.

Nian T K, Chen G Q, Luan M T, et al. Limit analysis of the stability of slopes reinforced with piles against landslide in nonhomogeneous and anisotropic soils[J]. Canadian Geotechnical Journal, 2008, 45(8): 1092-1103.

Pan Q, Xu J, Dias D. Three-dimensional stability of a slope subjected to seepage forces[J]. International Journal of Geomechanics, 2017, 17(8): 04017035.

Qi X H, Li D Q. Effect of spatial variability of shear strength parameters on critical slip surfaces of slopes[J]. Engineering Geology, 2018, 239: 41-49.

Srivastava A. Spatial variability modelling of geotechnical parameters and stability of highly weathered rock slope[J]. Indian Geotechnical Journal, 2012, 42(3): 179-185.

Sun Z, Li J, Pan Q, et al. Discrete kinematic mechanism for nonhomogeneous slopes and its application[J]. International Journal of Geomechanics, 2018, 18(12): 04018171.

Tabarroki M, Ahmad F, Banaki R, et al. Determining the factors of safety of spatially variable slopes modeled by random fields[J]. Journal of Geotechnical and Geoenvironmental Engineering, 2013, 139(12): 2082-2095.

Won J, You K, Jeong S, et al. Coupled effects in stability analysis of pile–slope systems[J]. Computers and Geotechnics, 2005, 32(4): 304-315.

Zhang J, Wang H, Huang H W, et al. System reliability analysis of soil slopes stabilized with piles[J]. Engineering geology, 2017, 229: 45-52.